EAST EUROPEAN JOURNAL OF PHYSICS. 3. 629-636 (2026)
DOI:10.26565/2312-4334-2026-3-58 ISSN 2312-4334

NANOPARTICLES AS PROBES OF THE ELECTRON ENERGY RELAXATION LENGTH IN A DC GLOW DISCHARGE

V. Lisovskiy*, S. Dudin, A. Shakhnazarian, S. Rezunenko
V.N. Karazin Kharkiv National University, 4 Svobody Sq., Kharkiv, 61022, Ukraine
**Corresponding Author email: lisovskiy@karazin.ua*
Received June 1, 2026; revised August 8, 2026; accepted August 23, 2026

A new method is proposed for determining the electron energy relaxation length in a DC glow discharge using nanoparticles as diagnostic probes. The method is based on nanoparticle confinement near the first field reversal point in the negative glow. At this position, a local maximum of the plasma potential forms a shallow potential pit for negatively charged nanoparticles. The position of the field reversal point can therefore be determined from the location of a nanoparticle cloud visualized by laser light scattering. Together with the measured cathode-layer thickness and the known interelectrode distance, this allows the electron energy relaxation length to be estimated using an analytical relation between these quantities. The method was demonstrated experimentally in an acetylene discharge, where nanoparticles are naturally formed by plasma polymerization. The electron energy relaxation length was found to increase, on average, with increasing discharge voltage. The experimentally estimated values were approximately 1.5 times larger than those calculated using an analytical model based on the first Townsend ionization coefficient. The discrepancy may partly result from the assumption of a constant electric field in the cathode layer adopted in the analytical model. The proposed method can also be extended to gases that do not form nanoparticles naturally by introducing preformed nanoparticles or by producing them initially in a suitable gas mixture.
Keywords: *Electron energy relaxation length; Nanoparticles; DC glow discharge; Potential pit; Ambipolar diffusion*

I. INTRODUCTION

In gas-discharge plasmas and plasma technologies, nonlocal heating of charged particles is often encountered, in which the regions where the particles gain high energy and where they dissipate this energy are spatially separated. For example, in negative ion sources [1–6], positive or negative ions extracted from the plasma are accelerated by an extractor and directed into a low-pressure gas volume (transport region) with no electric field, where they lose their energy through collisions with gas molecules.

In a DC discharge, electrons released from the cathode surface due to ion-induced electron emission gain considerable energy in the strong electric field of the cathode layer [7–15]. These electrons then leave the cathode layer and enter the negative glow, where the electric field is weak and may even reverse its direction. Since the electrons cannot gain energy in this region, they undergo elastic and inelastic collisions with gas molecules, lose the energy acquired in the cathode layer, and, in a sufficiently long discharge gap, eventually thermalize [16–20]. The distance over which this energy-loss process occurs is referred to as the electron energy relaxation length [7, 20]. Using known cross sections for electron collisions with gas molecules, the electron energy relaxation length can be calculated. However, even for an inert gas such as argon, the dependences of the energy relaxation length on electron energy calculated by different authors differ considerably, not only quantitatively but also qualitatively [18,19]. Therefore, it is useful to obtain at least an estimate of the electron energy relaxation length in various gases used in plasma technologies.

To our knowledge, micrometer-sized particles were first employed to estimate internal parameters of a gas-discharge plasma by the authors of Ref. [21], who used them to determine the electron temperature. Subsequently, charged micro- and nanoparticles have frequently been used to investigate electric fields in DC discharges and radio-frequency capacitively coupled discharges (see, for example, Ref. [22] and references therein).

Four different methods are commonly used to introduce nanoparticles into a gas discharge. Nanoparticles can be produced in advance, size-selected, and placed on an additional surface other than an electrode; a voltage pulse can then be applied in the plasma to lift the particles from the surface and form a nanoparticle cloud [23,24]. Alternatively, the cathode can be sputtered by ion bombardment in a DC discharge [25–29] or an arc discharge [30], with the sputtered atoms subsequently forming nano- and microparticles in the plasma. Preformed nanoparticles can also be introduced directly into the plasma volume using a dispenser [31–35]. Finally, a discharge can be generated in a gas whose molecules undergo dissociation to form monomers capable of producing nanoparticles through volume plasma polymerization [36–43].

DC glow discharges in acetylene are of interest for plasma processing because plasma polymerization leads to the deposition of carbon-containing films on electrode surfaces and discharge-tube walls [44–48]. By varying the discharge conditions, coatings ranging from polymer-like films to graphite [47] and even graphene [48] can be obtained. Of particular importance for the present work, however, is that under certain discharge conditions plasma polymerization also occurs in the plasma volume, resulting in the formation of nanoparticles [40].

Cite as: V. Lisovskiy, S. Dudin, A. Shakhnazarian, S. Rezunenko, East Eur. J. Phys. 3, 629 (2026), https://doi.org/10.26565/2312-4334-2026-3-58

These nanoparticles are formed predominantly in the negative glow and, after acquiring a negative charge, can be confined near the first field reversal point [7,40]. At this position, the local maximum of the plasma potential forms a shallow potential pit for negatively charged nanoparticles. The position of the first field reversal point is related to the energy relaxation of high-energy electrons emerging from the cathode layer into the negative glow. Therefore, the experimentally measurable position of the nanoparticle cloud can potentially be used as a diagnostic of the electron energy relaxation length.

In this work, we develop the physical basis of this diagnostic method and demonstrate it experimentally in a DC glow discharge in acetylene. The position of the nanoparticle cloud and the cathode-layer thickness are determined from discharge images and used to estimate the electron energy relaxation length. The obtained values are compared with those calculated using an analytical model based on the first Townsend ionization coefficient.

II. EXPERIMENTAL SETUP

The experimental setup used in this study is shown in Fig. 1. A cylindrical quartz discharge tube was positioned horizontally. Its inner diameter was 80 mm. Both electrodes were planar and made of stainless steel. The stationary cathode also served as a flange of the discharge tube and was supplied with a voltage of 0–1500 V from a power supply. The movable inner electrode served as a grounded anode. In the experiments reported in this work, the distance between the electrodes was fixed at 76.2 mm.

The experiments were performed in acetylene, which was introduced into the discharge chamber at a flow rate of up to 5 sccm (standard cubic centimeters per minute). Most experiments were carried out at a gas pressure of 0.2 Torr. The pressure was measured using a capacitance manometer (Baratron, MKS Instruments, USA) with an operating range from 1 mTorr to 1 Torr. A backing pump and a turbomolecular pump were used to evacuate the discharge chamber.

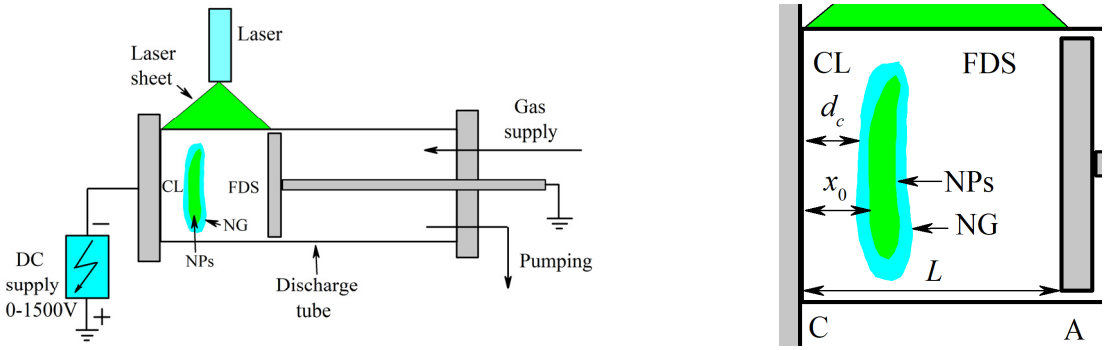

Figure 1. Schematic of the discharge chamber with a DC glow discharge

The nanoparticles are too small to be observed with the naked eye. Therefore, a green laser with a wavelength of 532 nm was used for their *in-situ* visualization. A cylindrical lens was used to split the laser beam into a light sheet, making it possible to observe a two-dimensional cross section of the nanoparticle cloud. This was sufficient for the purposes of the present study. If necessary, however, the three-dimensional shape of the cloud could also be determined by scanning it with the light sheet. Naturally, efficient light scattering by the nanoparticles requires sufficiently large particle sizes (several tens of nanometers or larger) as well as a sufficiently high nanoparticle concentration. These requirements determine the range of acetylene pressures investigated in this study (0.05–0.2 Torr). Under these conditions, nanoparticle formation and the increase in their size and number are sufficiently intense, while the DC discharge remains “short,” i.e., no positive column is formed. This issue is discussed in more detail below.

III. DC DISCHARGE STRUCTURE AND NANOPARTICLE FORMATION AND CONFINEMENT

In general, the DC discharge is one of the most extensively studied types of gas discharges. It is commonly generated in a cylindrical tube with planar electrodes located at its ends. After gas breakdown, a discharge with the following sequence of regions is formed. Adjacent to the cathode is the so-called cathode layer, across which a high voltage drop (several hundred volts or more) occurs. In Figs. 1 and 2, the cathode is denoted by C and the cathode layer by CL. The next region is the negative glow (NG), which gradually transits into the Faraday dark space (FDS). If the anode (A) is located within the Faraday dark space, such a discharge is conventionally referred to as a short discharge. In contrast, in a sufficiently long tube and/or at high gas pressure, a positive column and an anode layer with an anode glow may additionally appear. As mentioned above, all experiments were performed with a short discharge. Since the voltage drops across the negative glow and the Faraday dark space are small (several volts or less) [7,10,15,49], the voltage drop across the cathode layer can be considered approximately equal to the potential difference between the electrodes.

Figure 2 shows two photographs of the discharge. First, immediately after ignition, the discharge was photographed with the laser switched off [Fig. 2(a)]. The discharge structure described above, consisting of the cathode layer, negative glow, and Faraday dark space, can be clearly seen. When the light sheet is subsequently switched on, a

thin nanoparticle cloud appears in the negative glow after several seconds (or tens of seconds, depending on the gas pressure and the voltage between the electrodes), as indicated by NPs in Fig. 2(b). With time, the cloud may expand and become deformed [40], but in the present work we are specifically interested in the case of a thin nanoparticle cloud.

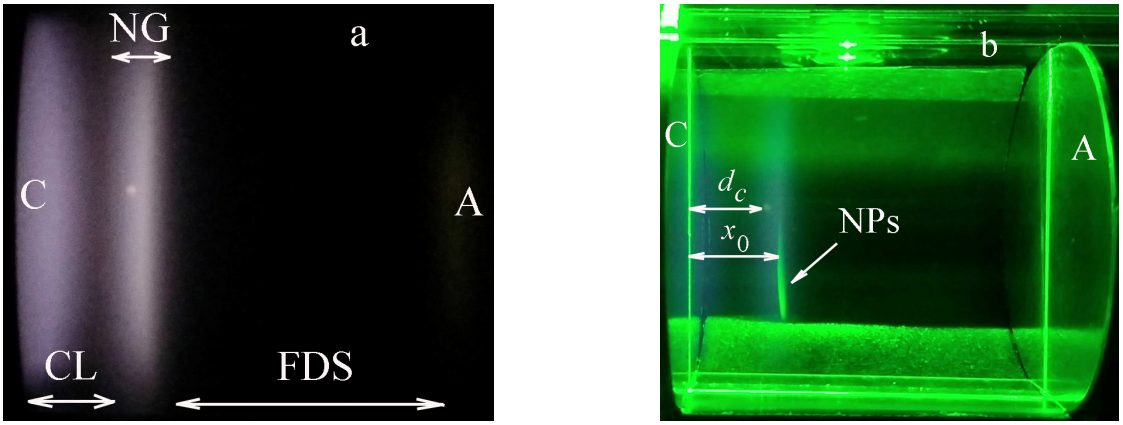

Figure 2. Photographs of the acetylene discharge at a pressure of 0.2 Torr with the light sheet (a) switched off and (b) switched on, at an interelectrode voltage of 440 V

To clarify why the nanoparticle cloud forms specifically in the negative glow, we consider the processes occurring in this region as well as in the cathode layer. Qualitative axial distributions of the electric field E, potential φ, positive ion density n_i, and electron density n_e in a short discharge are shown in Fig. 3.

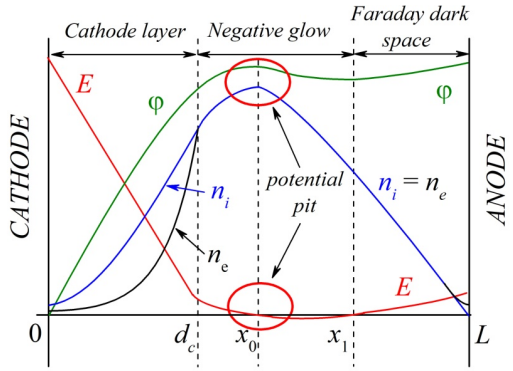

Figure 3. Axial distributions of the electric field E, potential φ, electron density n_e, and positive ion density n_i in a short discharge gap without a positive column

The cathode surface is bombarded by positive ions produced by ionization of acetylene molecules by high-energy electrons in the cathode layer and in the adjacent part of the negative glow. A strong electric field exists in the cathode layer. It reaches its maximum near the cathode surface and decreases almost linearly with increasing distance from the cathode. At the cathode-layer boundary ($x = d_c$), the electric field is small, but it reaches zero only within the negative glow, where the axial distributions of the electron and positive ion densities exhibit maxima, at a distance $x = x_0$ from the cathode. This position is referred to as the first field reversal point. The zero electric field means that the electrostatic potential reaches an extremum at this point, a maximum in the present case. For negatively charged particles, this local maximum of the electrostatic potential corresponds to a minimum of their potential energy and therefore forms a shallow potential pit in the vicinity of x_0. Its depth is usually small, less than 1 V [40]. A second field reversal point, at $x = x_1$, occurs near the boundary between the negative glow and the Faraday dark space.

Cold electrons and negatively charged nanoparticles can be confined in the shallow potential pit near the first field reversal point x_0. They cannot move toward the cathode because the strong electric field drives them back into the negative glow. Nor can they move toward the anode, because the electric field on the other side of x_0 drives them back. Therefore, the nanoparticle cloud initially formed in the negative glow is narrow and located near x_0. Naturally, when the nanoparticle concentration and particle size become sufficiently large, the cloud may broaden due to deformation of the potential pit by the charged nanoparticles [40]. In the present work, however, we consider specifically the case of a thin nanoparticle cloud.

Electrons are emitted from the cathode surface due to ion-induced electron emission and enter the strong electric field of the cathode layer. As they travel through the layer, they acquire considerable energy and ionize gas molecules. Some electrons emitted from the cathode or produced by ionization near its surface can traverse almost the entire cathode layer with little energy loss, undergoing only one or a few inelastic collisions with gas molecules, and

consequently acquire high energies approaching $e \cdot U_c$, where e is the elementary charge and U_c is the voltage drop across the cathode layer. A flux of such high-energy electrons therefore emerges from the cathode layer into the negative glow. There, these electrons begin to lose energy intensively through collisions with gas molecules, exciting their electronic states and ionizing them. As a result, a bright negative glow is observed; its intensity maximum coincides with the maximum plasma density, where the electric field reaches zero and reverses its direction.

High-energy electrons not only ionize and excite gas molecules. Collisions of these electrons with acetylene molecules may lead to dissociation with the formation of C_2H radicals, as well as to dissociative electron attachment resulting in the formation of C_2H^- negative ions. These C_2H and C_2H^- species can combine with C_2H_2 molecules to form more complex molecules; thus, they effectively act as monomers capable of forming long polymer chains. A list of the corresponding reactions is given, for example, in Ref. [40]. As these reactions continue, nanoparticles are eventually formed.

In general, the negative glow is an optimal region of a DC discharge for nanoparticle formation and confinement. It contains fluxes of high-energy electrons capable of producing C_2H and C_2H^-. At the same time, it contains a potential pit for negatively charged nanoparticles and negative ions, provided that negative ions can be formed in the gas under investigation.

An additional requirement of our method is the horizontal orientation of the discharge tube containing vertically oriented planar electrodes. If the electrodes are horizontal and the cathode is located at the bottom, sufficiently large nanoparticles are not confined at the first field reversal point x_0; instead, gravity causes them to settle toward the cathode-layer boundary or even penetrate slightly into the cathode layer. If the anode is located at the bottom, the nanoparticles formed in the plasma cannot be confined by the shallow potential pit [40] and fall onto the anode surface [50]. With horizontal electrodes, the nanoparticles are confined in the plasma by the axial electric field responsible for carrying the discharge current.

In our discharge chamber with vertically oriented electrodes, however, the situation is different. The axial electric field is now directed horizontally, whereas gravity acts vertically. The nanoparticles are confined in the plasma volume by the radial ambipolar electric field that arises because a fraction of the high-energy electrons escapes to the tube wall. The wall becomes negatively charged and repels cold electrons back into the plasma. At the same time, a small flux of positive ions reaches the wall from the plasma, accompanied by an equally small flux of high-energy electrons. Therefore, unlike the axial electric field, the ambipolar electric field does not carry the discharge current [49].

The accumulation of negative ions and negatively charged nanoparticles in the plasma leads to a substantial reduction in the ambipolar electric field [51-55]. At sufficiently high concentrations, the field may decrease to zero and even reverse its direction [56]. More generally, the presence of negative ions, in addition to electrons and positive ions, can substantially affect the structure and properties of discharge plasmas [57-68]. Negative ions are produced by electron attachment to gas molecules [49]; this process therefore results in the loss of free electrons that would otherwise ionize gas molecules and carry the discharge current.

IV. METHOD FOR DETERMINING THE ELECTRON ENERGY RELAXATION LENGTH USING NANOPARTICLES

We now consider how nanoparticles synthesized in a DC discharge can be used as a diagnostic tool for estimating the energy relaxation length of electrons that travel from the cathode surface to the cathode-layer boundary with almost no collisions with gas molecules and, consequently, lose little energy. Such electrons have high energies, which can reach $e \cdot U_c$, where U_c is the voltage drop across the cathode layer. These electrons are responsible for the ionization of gas molecules and for sustaining the discharge, and they also carry a substantial fraction of the discharge current through the negative glow [16,17].

As shown experimentally above, the nanoparticle cloud forms and is confined in the negative glow near the so-called first field reversal point, located at a distance x_0 from the cathode. We now consider the location of the first field reversal point shown in Fig. 3. J. P. Boeuf and L. C. Pitchford [7] proposed an analytical model of a DC glow discharge and obtained the following expression for the position of the field reversal:

$$\frac{x_0 - d_c}{L - d_c} = -\Lambda \cdot ln\left[\Lambda \cdot \left(1 - \mathrm{e}^{-1/\Lambda}\right)\right], \tag{1}$$

where L is the distance between the electrodes, $\Lambda = \lambda/(L - d_c)$, and λ is the distance over which the energy relaxation of electrons accelerated in the cathode layer and entering the negative glow occurs.

Equation (1) can readily be rewritten as

$$x_0 = d_c - \lambda \cdot ln\left[\frac{\lambda}{L - d_c} \cdot \left(1 - exp\left(-\frac{L - d_c}{\lambda}\right)\right)\right]. \tag{2}$$

Subsequently, in analytical models of a DC glow discharge, the authors of Ref. [20] obtained the same expression, Eq. (2), but for the position of the maximum plasma density in the negative glow. We therefore conclude that the field reversal occurs at the position where the plasma density reaches its maximum.

Since the interelectrode distance L is known, while the cathode-layer thickness d_c and the coordinate of the first field reversal point x_0 can be determined from photographs of the discharge, Eq. (2) can be used to estimate the electron energy relaxation length λ. The corresponding results for an acetylene pressure of 0.2 Torr are shown in Fig. 4. Both the cathode-layer thickness d_c and the coordinate of the first field reversal point x_0 decrease monotonically with increasing voltage between the electrodes. The electron energy relaxation lengths λ obtained in the present work are shown by solid blue squares. On average, λ increases monotonically with the voltage U.

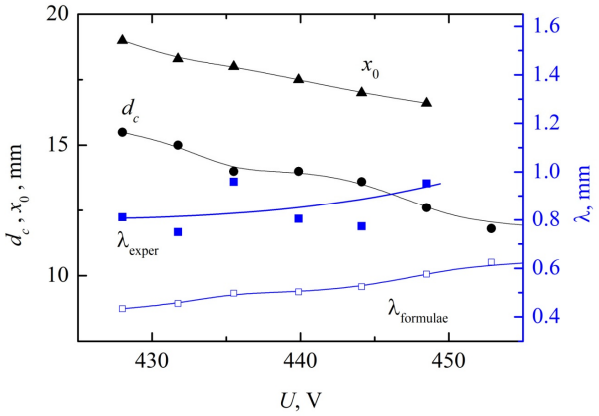

Figure 4. Cathode-layer thickness d_c, coordinate of the first field reversal point x_0, and electron energy relaxation length λ as functions of the interelectrode voltage U at an acetylene pressure of 0.2 Torr. Solid blue squares show the values obtained in the present work; open blue squares show the values calculated using Eq. (3) [20]

The authors of Ref. [20] obtained the following expression for λ:

$$\lambda = \frac{U_c - Bpd_c}{\alpha_{CF} Bpd_c}, \tag{3}$$

where α_{CF} is the first Townsend ionization coefficient, for which Ref. [20] proposed the following expression:

$$\alpha_{CF} = Ap \cdot exp\left(-\frac{Bpd_c}{U_c}\right). \tag{4}$$

Thus, the authors of Ref. [20] assumed that, in the strong electric field of the cathode layer, the ionization rate is determined by the potential difference traversed by the electrons rather than by the local electric field. Therefore, Eqs. (3) and (4) use the average electric field in the cathode layer, U_c/d_c.

We recall that all experiments were performed under conditions where no positive column was present in the DC glow discharge. Since the voltage drops across the negative glow and the Faraday dark space are very small compared with the voltage drop U_c across the cathode layer, for the purposes of our estimates we can assume that U_c is equal to the voltage U between the electrodes, which can be readily measured.

It remains to determine the constants A and B to be used in Eq. (4) for acetylene. For this purpose, we used the BOLSIG+ code [69] with electron–acetylene collision cross sections from Refs. [70,71]. The resulting values of the first Townsend ionization coefficient are shown in Fig. 5 by solid circles and are well approximated by the following expression:

$$\alpha = 33 \cdot p \cdot exp\left(-\frac{450}{E/p}\right). \tag{5}$$

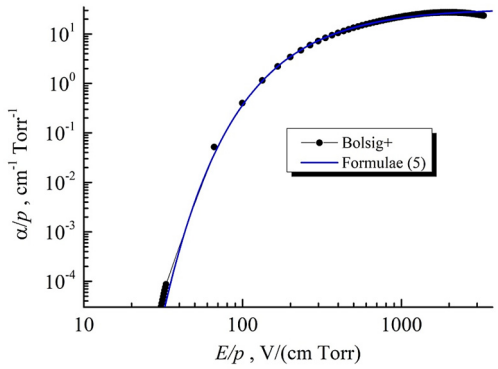

Figure 5. Ratio of the first Townsend ionization coefficient α to the gas pressure p, as a function of the reduced electric field E/p for acetylene. Solid circles show the results calculated using the BOLSIG+ code; the blue line represents the approximation given by Eq. (5)

Thus, the constants $A = 33$ cm^{-1} Torr^{-1} and $B = 450$ V/(cm Torr) should be used in Eq. (4). These constants were then substituted into Eqs. (3) and (4), and the calculated results were added to Fig. 4 as open blue squares. As can be seen from the figure, the experimentally estimated electron energy relaxation lengths λ are approximately 1.5 times larger than the values calculated using Eq. (3). However, that equation was derived assuming a constant electric field in the cathode layer, i.e., a linear potential profile across the layer, which is a rather crude approximation.

V. CONCLUSIONS

In this work, we developed the physical basis of a new method for determining the electron energy relaxation length in a DC glow discharge using nanoparticles as diagnostic probes. In a horizontal discharge tube with vertically oriented electrodes, nanoparticles can be confined in the negative glow near the first field reversal point. The local maximum of the plasma potential at this position forms a shallow potential pit for negatively charged nanoparticles. Since the coordinate of the nanoparticle cloud can be determined experimentally using laser light scattering, it provides a direct measure of the position of the first field reversal point. Combined with the measured cathode-layer thickness and the known interelectrode distance, this coordinate makes it possible to estimate the electron energy relaxation length using an analytical relation between these quantities.

The method was demonstrated experimentally for a DC glow discharge in acetylene, where nanoparticles are formed naturally as a result of plasma polymerization. The cathode-layer thickness and the position of the nanoparticle cloud were determined from discharge images over a range of discharge voltages, and the corresponding electron energy relaxation lengths were obtained. The estimated relaxation length increased with increasing discharge voltage. For comparison, the electron energy relaxation length was also calculated using an analytical model based on the first Townsend ionization coefficient. The required Townsend coefficients for acetylene were obtained using BOLSIG+ and approximated by the conventional exponential dependence on the reduced electric field. The experimentally estimated electron energy relaxation lengths were approximately 1.5 times larger than those predicted by the analytical model. This difference may be attributed, at least in part, to the assumption of a constant electric field in the cathode layer used in the analytical model, whereas the actual electric field varies substantially across the layer.

The proposed method is not restricted to gases in which nanoparticles are formed naturally. Nanoparticles can first be produced in a suitable gas mixture and subsequently retained in the discharge after the nanoparticle-forming component is removed. Alternatively, preformed nanoparticles can be introduced into the plasma from an external source. Once negatively charged and confined near the first field reversal point, the nanoparticles can serve as probes of its position. Thus, the proposed approach can potentially be used to estimate the electron energy relaxation length in a wide range of gases employed in low-pressure plasma applications.

ORCID

V. Lisovskiy, https://orcid.org/0000-0002-6339-4516; **S. Dudin,** https://orcid.org/0000-0001-9161-4654;
A. Shakhnazarian, https://orcid.org/0009-0000-2951-0969; **S. Rezunenko,** https://orcid.org/0009-0001-5871-495X

REFERENCES

[1] I. Sereda, Y. Hrechko, I. Babenko, and M. Azarenkov, Vacuum, **200**, 111006 (2022). https://doi.org/10.1016/j.vacuum.2022.111006
[2] M. Bacal, editor, *Physics and Applications of Hydrogen Negative Ion Sources* (Springer, Cham, Switzerland, 2023). https://doi.org/10.1007/978-3-031-21476-9
[3] I. Sereda, Y. Hrechko, and M. Azarenkov, Phys. Plasmas **31**, 053516 (2024). https://doi.org/10.1063/5.0202579
[4] L. Yang, Y. Xie, X. Peng, D. S. Stepanov, J. Pan, and Ch. Hu, Phys. Plasmas **32**, 033510 (2025). https://doi.org/10.1063/5.0249289
[5] I. Sereda, Y. Hrechko, M. Azarenkov, and K. Sereda, Intern. J. Hydrogen Energy, **109**, 1321 (2025). https://doi.org/10.1016/j.ijhydene.2025.02.222
[6] I. Sereda, Y. Hrechko, K. Sereda, and O. Vorobiov, East European Journal of Physics **2**, 470 (2026). https://doi.org/10.26565/2312-4334-2026-2-52
[7] J. P. Boeuf, and L. C. Pitchford, J. Phys. D: Appl. Phys. **28**, 2083 (1995). https://doi.org/10.1088/0022-3727/28/10/013
[8] K. Rózsa, A. Gallagher, and Z. Donkó, Physical Review E **52**, 913 (1995). https://doi.org/10.1103/PhysRevE.52.913
[9] C.V. Budtz-Jørgensen, J. Bøttiger, and P. Kringhøj, Vacuum **56**, 9 (2000). https://doi.org/10.1016/S0042-207X(99)00160-8
[10] V.A. Lisovskiy, and S.D. Yakovin, Technical Physics Letters 26, 891 (2000). https://doi.org/10.1134/1.1321230
[11] Z. Donkó, J. Appl. Phys. **88**, 2226 (2000). https://doi.org/10.1063/1.1288008
[12] V.A. Lisovskiy, V.A. Derevianko, and V.D. Yegorenkov, Vacuum **103**, 49 (2014). https://doi.org/10.1016/j.vacuum.2013.12.008
[13] A. Michau, G. Lombardi, L. Colina Delacqua, M. Redolfi, C. Arnas, P. Jestin, X. Bonnin, and K. Hassouni, Plasma Chem. Plasma Process 32,451 (2012). https://doi.org/10.1007/s11090-012-9357-0
[14] Y. Y. Lau, D. Li, and D. P. Chernin, Phys. Plasmas **30**, 093104 (2023). https://doi.org/10.1063/5.0169276
[15] V. Lisovskiy, S. Dudin, A. Shakhnazarian, S. Rezunenko, V. Yegorenkov, Phys. Plasmas **32**, 083501 (2025). https://doi.org/10.1063/5.0275627
[16] L. D. Tsendin, Physics-Uspekhi **53**, 133 (2010). https://doi.org/10.3367/UFNe.0180.201002b.0139
[17] V. A. Lisovskiy, K. P. Artushenko, and V. D. Yegorenkov, Phys. Plasmas, **24,** 053501 (2017). https://doi.org/10.1063/1.4982211

[18] S. Siepa, S. Danko, T.V. Tsankov, Th. Mussenbrock, and U. Czarnetzki, J. Phys. D: Appl. Phys. **47**, 445201 (2014). https://doi.org/10.1088/0022-3727/47/44/445201
[19] C. Yuan, J. Yao, E.A. Bogdanov, A.A. Kudryavtsev, K.M. Rabadanov, and Z. Zhou, Phys. Plasmas **26**, 023509 (2019). https://doi.org/10.1063/1.5082698
[20] A. A. Kudryavtsev, A. V. Morin, and L. D. Tsendin, Tech. Phys. **53**, 1029 (2008). https://doi.org/10.1134/S1063784208080100
[21] T. C. Anestos, and C. D. Hendricks, J. Appl. Phys. **45**, 1176 (1974). https://doi.org/10.1063/1.1663385
[22] J. C. A. van Huijstee, L. S. Matthews, and T. W. Hyde, Phys. Plasmas **32**, 113703 (2025). https://doi.org/10.1063/5.0287405
[23] E. Thomas, IEEE Trans. Plasma Sci. **30**, 88 (2002). https://doi.org/10.1109/TPS.2002.1003937
[24] E. Thomas, Phys. Scripta **2001**, 20 (2006). https://doi.org/10.1238/Physica.Topical.089a00020
[25] G. M. Jellum, and D. B. Graves, J. Appl. Phys. **67**, 6490 (1990). https://doi.org/10.1063/1.346081
[26] C. Dominique, and C. Arnas, J. Appl. Phys. **101**, 123304 (2007). https://doi.org/10.1063/1.2748365
[27] C. Arnas, A. Michau, G. Lombardi, L. Couëdel, and K. Kishor Kumar, Phys. Plasmas **20**, 013705 (2013). https://doi.org/10.1063/1.4776681
[28] K. Kishor Kumar, L. Couëdel, and C. Arnas, Phys. Plasmas **20**, 043707 (2013). https://doi.org/10.1063/1.4802809
[29] S. Barbosa, F. R. A. Onofri, L. Couëdel, M. Wozniak, C. Montet, C. Pelcé, C. Arnas, L. Boufendi, E. Kovacevic, J. Berndt, and C. Grisolia, J. Plasma Phys. **82**, 615820403 (2016). https://doi.org/10.1017/S0022377816000714
[30] I. Langmuir, C. G. Found, and A. F. Dittmer, Science **60**, 392 (1924). https://doi.org/10.1126/science.60.1557.392
[31] J. Niemann, V. Schneider, and H. Kersten, Phys. Plasmas **32**, 013510 (2025). https://doi.org/10.1063/5.0243765
[32] P. Gogoi, B. Chutia, P. Sut, Y. Bailung, N. C. Adhikary, and H. Bailung, Phys. Plasmas **31**, 023706 (2024). https://doi.org/10.1063/5.0177617
[33] L. Wimmer, A.S. Schmitz, M. Kretschmer, and M.H. Thoma, Phys. Plasmas **31**, 043702 (2024). https://doi.org/10.1063/5.0190499
[34] J. Goswami, N. Das, D. Goswami, S.S. Kausik, and B.K. Saikia, Phys. Plasmas **33**, 013701 (2026). https://doi.org/10.1063/5.0306369
[35] J. C. A. van Huijstee, L. S. Matthews, and T. W. Hyde. Phys. Plasmas **32**, 113703 (2025). https://doi.org/10.1063/5.0287405
[36] A. R. Westwood, European Polymer Journal **7**, 377 (1971). https://doi.org/10.1016/0014-3057(71)90008-5
[37] R. Liepins, and K. Sakaoku, J. Appl. Polym. Sci. **16**, 2633 (1972). https://doi.org/10.1002/app.1972.070161016
[38] V. Lisovskiy, A. Minenkov, S. Dudin, S. Bogatyrenko, P. Platonov, and V. Yegorenkov, ACS Omega 7, 47941 (2022). https://doi.org/10.1021/acsomega.2c05846
[39] L. Worner, E. Kovacevic, J. Berndt, H. M. Thomas, M. H. Thoma, L. Boufendi, and G. E. Morfill, New Journal of Physics **14**, 023024 (2012). https://doi.org/10.1088/1367-2630/14/2/023024
[40] V. Lisovskiy, S. Dudin, S. Bogatyrenko, A. Shakhnazarian, and S. Rezunenko, Phys. Plasmas **33**, 083704 (2026); https://doi.org/10.1063/5.0326778
[41] J. Winter, J. Berndt, S.-H. Hong, E. Kovacevic, I. Stefanovic, and O. Stepanovic, Plasma Sources Sci. Technol. **18**, 034010 (2009). https://doi.org/10.1088/0963-0252/18/3/034010
[42] E. Kovacevic, J. Berndt, Th. Strunskus, and L. Boufendi, J. Appl. Phys. **112**, 013303 (2012). https://doi.org/10.1063/1.4731751
[43] E. Kovačević, J. Berndt, I. Stefanović, H.-W. Becker, C. Godde, Th. Strunskus, J. Winter, and L. Boufendi, J. Appl. Phys. **105**, 104910 (2009). http://dx.doi.org/10.1063/1.3129318
[44] S.M. Miladinović, V. Vriendt, S. A. Robotham, F. Maseri, S. Lucas, and C.L. Wilkins, J. Am. Soc. Mass Spectrometry **21**, 411 (2010). https://doi.org/10.1016/j.jasms.2009.11.005
[45] A. Moshonov, and Y. Avny, J. Appl. Polymer Sci. **25**, 771 (1980). https://doi.org/10.1002/app.1980.070250506
[46] B. Alvarez, A. Sarmiento-Santos, and E. Vera-López, J. Phys.: Conf. Series **1386**, 012044 (2019). https://doi.org/10.1088/1742-6596/1386/1/012044
[47] B. Alvarez, A. Sarmiento-Santos, and Y. Hernandez, J. Phys.: Conf. Series **1386**, 012042 (2019). https://doi.org/10.1088/1742-6596/1386/1/012042
[48] B. Alvarez, A. Sarmiento-Santos, and Y. Hernandez, J. Phys.: Conf. Series **1386**, 012014 (2019). https://doi.org/10.1088/1742-6596/1386/1/012014
[49] Yu. P. Raizer, *Gas discharge physics*, (Springer, Berlin, 1991).
[50] L. Couëdel, K. Kishor Kumar, and C. Arnas, Phys. Plasmas **21**, 123703 (2014). https://doi.org/10.1063/1.4903465
[51] J. B. Thompson, Proc. Phys. Soc. **73**, 818 (1959). https://doi.org/10.1088/0370-1328/73/5/416
[52] A. J. Lichtenberg, V. Vahedi, M. A. Lieberman, and T. Rognlien, J. Appl. Phys. **75**, 2339 (1994). https://doi.org/10.1063/1.356252
[53] E. Stoffels, W. W. Stoffels, D. Vender, M. Haverlag, G. M. W. Kroesen, and F. J. de Hoog, Contrib. Plasma Phys. **35**, 331 (1995). https://doi.org/10.1002/ctpp.2150350404
[54] Y. T. Lee, M. A. Lieberman, A. J. Lichtenberg, F. Bose, H. Baltes, and R. Patrick, J. Vac. Sci. Technol. A **15**, 113 (1997). https://doi.org/10.1116/1.580452
[55] V. Lisovskiy, and V. Yegorenkov, Europhysics Letters **99**, 35002 (2012). https://doi.org/10.1209/0295-5075/99/35002
[56] V. Lisovskiy, S. Dudin, S. Bogatyrenko, S. Rezunenko, and V. Yegorenkov, East European Journal of Physics **2**, 445 (2026). https://doi.org/10.26565/2312-4334-2026-2-50
[57] M. Mao, J. Benedikt, A. Consoli, and A. Bogaerts, J. Phys. D: Appl. Phys. **41**, 225201 (2008). https://doi.org/10.1088/0022-3727/41/22/225201
[58] S. V. Dudin, S. D. Yakovin, and A. V. Zykov, East European Journal of Physics **3**, 606 (2023). https://doi.org/10.26565/2312-4334-2023-3-72
[59] V. O. Litvinov, I. I. Okseniuk, D. I. Shevchenko, and V. V. Bobkov, East European Journal of Physics **3**, 10 (2023). https://doi.org/10.26565/2312-4334-2023-3-01
[60] V. Lisovskiy, S. Dudin, A. Shakhnazarian, P. Platonov, and V. Yegorenkov, East European Journal of Physics **3**, 172 (2024). https://doi.org/10.26565/2312-4334-2024-3-17

[61] T. Wang, Sh. Rauf, N. Friedrichs, I. Korolov, J. Kenney, and J. Schulze, Phys. Plasmas 33, 023501 (2026) https://doi.org/10.1063/5.0300388
[62] X. K. Wang, R. Masheyeva, Y. X. Liu, Y. H. Song, P. Hartmann, Z. Donko, and J. Schulze, Plasma Sources Sci. Technol. **33**, 085006 (2024). https://doi.org/10.1088/1361-6595/ad69c0
[63] R. Masheyeva, M. Vass, M. Myrzaly, C.-B. Tian, K. Dzhumagulova, J. Schulze, Z. Donko, and P. Hartmann, Plasma Sources Sci. Technol. **34**, 045017 (2025). https://doi.org/10.1088/1361-6595/adcb6b
[64] H. Luo, J. Kenney, S. Rauf, I. Korolov, and J. Schulze, Plasma Sources Sci. Technol. **32**, 115018 (2023). https://doi.org/10.1088/1361-6595/ad0d06
[65] A. Derzsi, M. Vass, R. Masheyeva, B. Horvath, Z. Donko, and P. Hartmann, Plasma Sources Sci. Technol. **33**, 025005 (2024). https://doi.org/10.1088/1361-6595/ad1fd5
[66] J. Sangma, N. Sharma, M. Chakraborty, and M. Bandyopadhyay, Phys. Plasmas **29**, 033501 (2022). https://doi.org/10.1063/5.0078194
[67] G.-H. Huang, S.-Y. Xing, F. Gao, and Y.-N. Wang, Phys. Plasmas **32**, 123507 (2025). https://doi.org/10.1063/5.0300603
[68] I. Tanarro, R. J. Peláez, and V. J Herrero, Plasma Phys. Control. Fusion **67**, 035014 (2025). https://doi.org/10.1088/1361-6587/adb17b
[69] G.J.M. Hagelaar, and L.C. Pitchford, Plasma Sources Sci. Technol. **14**, 722 (2005). https://doi.org/10.1088/0963-0252/14/4/011
[70] L.C. Pitchford, L.L. Alves, K. Bartschat, S.F. Biagi, M.C. Bordage *et al*, Plasma Process. Polym. 14, 1600098 (2017). https://doi.org/10.1002/ppap.201600098
[71] M. Hayashi, *Electron collision cross sections determined from beam and swarm data by Boltzmann analysis*, in *Nonequilibrium Processes in Partially Ionized Gases*, edited by M. Capitelli, and J.N. Bardsley, (Plenum Press, New York, 1990). https://doi.org/10.1007/978-1-4615-3780-9

НАНОЧАСТИНКИ ЯК ЗОНДИ ДЛЯ ВИЗНАЧЕННЯ ДОВЖИНИ РЕЛАКСАЦІЇ ЕНЕРГІЇ ЕЛЕКТРОНІВ У ТЛІЮЧОМУ РОЗРЯДІ ПОСТІЙНОГО СТРУМУ

В. Лісовський, С. Дудін, А. Шахназарян, С. Резуненко
Харківський національний університет імені В.Н. Каразіна, майдан Свободи 4, Харків, 61022, Україна

Запропоновано нову методику визначення довжини релаксації енергії електронів у тліючому розряді постійного струму з використанням наночастинок як діагностичних зондів. Методика ґрунтується на утриманні наночастинок поблизу першої точки зворотності електричного поля в негативному світінні. У цій області локальний максимум потенціалу плазми утворює потенціальну яму для негативно заряджених наночастинок. Таким чином, положення точки зворотності електричного поля можна визначити за розташуванням хмари наночастинок, яку було візуалізовано за допомогою розсіювання лазерного випромінювання. Разом із виміряною товщиною катодного шару та відомою відстанню між електродами це дозволяє оцінити довжину релаксації енергії електронів за допомогою аналітичного співвідношення між цими величинами. Методику експериментально продемонстровано в розряді в ацетилені, де наночастинки природним чином утворюються внаслідок плазмової полімеризації. Встановлено, що в середньому довжина релаксації енергії електронів збільшується зі зростанням напруги розряду. Експериментально оцінені значення виявилися приблизно в 1,5 раза більшими за значення, розраховані за допомогою аналітичної моделі, що ґрунтується на першому коефіцієнті іонізації Таунсенда. Ця розбіжність може бути частково зумовлена припущенням про постійну напруженість електричного поля в катодному шарі, прийнятим в аналітичній моделі. Запропоновану методику також можна поширити на гази, в яких наночастинки природним чином не утворюються, шляхом введення попередньо сформованих наночастинок або їх початкового формування у відповідній газовій суміші.

Ключові слова: *довжина релаксації енергії електронів; наночастинки; розряд постійного струму; потенціальна яма; амбіполярна дифузія*